

MAT GLASS – THIN LAYER CHROMATOGRAPHY. APPLICATION OF INVASION MODEL

Mihaela VLASSA^a, Miuța FILIP^{a,*}, Ștefan KREIBIK^a,
Diana BOGDAN^b, Virginia COMAN^a

ABSTRACT. This study presents the theoretical and practical aspects of the new technique, namely Mat Glass - Thin Layer Chromatography (MG-TLC) and application of invasion model. Our research is focused on the development and clarification of the phenomena that occur in thin layer separation technique: process flow, spreading on mat glass surface, impregnation of porous layers and the improvement of the quality of thin layer chromatographic separations by overlapping some mat glass plates, over the chromatographic plates. The experiments have confirmed the possibility that the movement of the invasive type displacement, which occurs on rough surface will influence favorably the chromatographic separation processes. Good results have been obtained in separation of the lipophilic dyes and the hydrophilic dyes by small adjustments, e.g., height of the free zone of porous layer h , or the roughness of glass plates. The results obtained demonstrate that this method can be successfully used in thin layer chromatography technique being easy to apply and inexpensive compared with other methods derived from chromatography.

Keywords: *Capillarity, Invasive model, Mat Glass, Thin Layer Chromatography.*

INTRODUCTION

During the lately decades efforts have been done to improve and diversify the Thin Layer Chromatography (TLC) technique regarding the quality of separations, analysis speed, widen the range of substances that can be separated

^a Babeș-Bolyai University, Raluca Ripan Institute for Research in Chemistry, 30 Fântânele Street, 400294 Cluj-Napoca, Romania

^b National Institute for Research and Development of Isotopic and Molecular Technologies, 67-103 Donath Street, 400293 Cluj-Napoca, Romania

* Corresponding author: miuta.filip@ubbcluj.ro



by this technique and lower costs. Also, under certain conditions in TLC, some processes such as: exposure to the vapor atmosphere of the TLC plate, different speed of the eluent, the design of chromatographic chambers can determine a great influence on the separations process, on the analysis time and on research funding costs [1].

There are a few vectors that were used in combination with the principle of TLC like: the centrifugal force in so-called rotation planar chromatography [1]; the electric fields exterior to the TLC plate generated by the continuous electrical voltage [2]; the exterior electric fields to the TLC plate namely: non-uniform, alternatives, high voltage, audio frequency or pulsating [3,4,5]; the application of magnetic fields [6,7]; the pressure applied to the eluent flow at OPLC technique [8,9].

Another category for enhancement of the TLC technique aimed the following three aspects:

(1) Reducing the granulation of porous medium particles. OPLC technique use micro particles with effect on improving the quality of separation, including reducing analysis time [8,9]. A very good separation was obtained by using the stationary phase with micro particles under 2 μm [10];

(2) Changes in the composition of the alumina by increasing amounts of BaTiO₃ showed that the TLC quality of separation was improved [6,11];

(3) Study of the influence of vapors of mobile phase on the chromatographic process [12,14] and on a sandwich type device for TLC with a closed adsorbent layer [13].

Some of the TLC methods listed above, lead to costly interventions more [8,9] or less [13,14] but all these improved methods aim at raising the quality of the separation, improving the applications TLC method by diversification of substances able to be separated and lowering the prices.

In this paper we studied some theoretical and practical aspects of MG-TLC technique by investigation of process flow, spreading on mat glass surface, impregnation of porous layers, in chromatographic separations of the lipophilic dyes and the hydrophilic dyes.

RESULTS AND DISCUSSION

Theoretical aspects of MG-TLC technique

Chromatographic separation processes in TLC consist mainly of repeated balance of the adsorption of the solute between the porous medium and solvent molecules. Finally, distinct spots are filled separately from each other on the TLC plate. The separation phenomenon is very complex and depends on a lot of

factors such as: type of the adsorbent used, eluent type or eluent mixture used, eluent speed, the physical-chemical properties of the porous adsorbent medium (porosity, grain size, specific surface area, etc.). Also, the exterior conditions offered to chromatographic analysis influences the separation: TLC chamber volume, vapor chamber saturation, ambient temperature, the number of successive separations made on the plate, input position of the eluent in the TLC plate (from the top or bottom, for example), type of the used chromatography: adsorption, repartition, etc. [1-3].

In the first phase, by using TLC commercial plates it was studied the influence of some parameters, mentioned above by applying on the adsorbent surface a mat glass plate in the manner presented by Berezkin [13] and Bauer [14]. The Figure 1 shows the sandwich type device used for MG-TLC experiments and a detail of the inferior part.

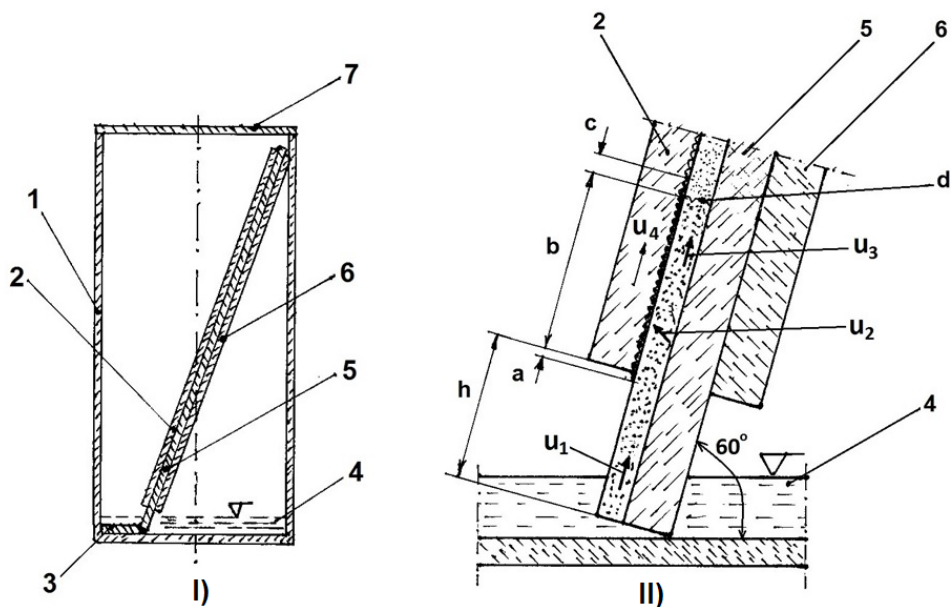


Figure 1. Section sketch of the Mat-Glass Thin Layer Chromatographic sandwich device (I) with a detail of the inferior part (II).

1 - chromatographic standard chamber; 2 - mat glass plate; 3 - movement limiter; 4 - eluent; 5 - TLC plate; 6 - counter plate; 7 - lid; Note: retaining clips of the plates 2, 5 and 6 are not drawn. a - meniscus input; b - mesoscopic fluid invasion regime; c - precursor film; d - total meniscus (currently) in porous media; h - the free zone of porous layer; u_1 - eluent speed in the free zone; u_2 - the speed of the eluent in the porous media toward the mat glass plate; u_3 - momentary speed of the eluent through porous medium; u_4 - invasive momentary speed of the eluent on the surface of the mat plate (2).

The work experiments, revealed that u_3 and u_4 have equal speed, the front of the menisci from the porous medium (denoted d) as well as the front on the rough matt plate, coincide with mutual conditionality. The cause of these conditions are the forces of cohesion between the two tides of fluids, these forces being described by Gregg [15]. On the h free zone, the evaporation speed of eluent was neglected, even if eluent evaporation has a great importance in the adjustment of the eluent flow in sandwich chamber and in regulate of u_1 , u_2 , u_3 and u_4 speeds. It was considered to be necessary to express the eluent speed in the two layers, porous and mat plate surfaces.

Eluent flow through porous medium

The basis for most treatments on absorbency and wicking flows is the Washburn equation (Equation 1) [16]:

$$\zeta = kt^{1/2} \quad (1)$$

Here ζ is the depth of fluid penetration and k is a constant (Equation 2) that has the following form for Poiseuille flow in a cylindrical, horizontally oriented capillary of radius r :

$$k = \left[\frac{r\sigma\cos\theta}{2\mu} \right]^{1/2} \quad (2)$$

Where, σ is the liquid surface tension and μ is its viscosity.

A similar relationship used in chromatography, among others, proposed by Guiochon (Equation 3) [17] is:

$$z_f^2 = kt \quad (3)$$

where the constant k is a function of the nature of the chromatographic system and of the dimension of the bed particles, z_f is the distance between the solvent front and the solvent source.

A liquid enters a capillary because this decreases its free energy. The change in free energy is inversely proportional to the capillary radius, so the liquid will fill the narrowest capillaries available first [17]. Following we used the relationships calculated by Belenkii [18] and adapted by Guiochon [17] for eluent front velocity u (Equation 4):

$$u = \frac{k_o d_p \gamma \cos\theta}{\eta z_f} \quad (4)$$

where: d_p is the particle diameter of porous bed; γ is the surface tension of the mobile phase; θ is the surface contact angle of solvent with the adsorbent; η is the solvent viscosity; z_f is the distance of migration, and

$$k_o = \frac{\varepsilon_l^3}{180(1-\varepsilon_l)^2} \quad (5)$$

where ε_l is the external bed porosity (volume of interparticle space/volume of bed).

In Equation 4 it can be observed that the relationship between eluent front velocity u and its movement z is not strictly linear because of k_o that are changed with the change of ε_l porosity. This porosity changes in time, as the solvent vapour from TLC chamber is adsorbed on the surface of the pores, causing the narrowing capillaries. The same equation of the speed solvent front was used by Poole [19].

Eluent transfer and flow on the surface of the mat glass plate

The transfer of liquid on the surface of a rough glass plate follows two mechanisms: (1) by contact of the rough surface prominences with the surface of TLC plate; (2) by solvent evaporation transported through the porous medium of the TLC plate and by condensation of vapor on the above surface the rough plate.

Wåhlander et al. [20] and Hansson et al. [21] have dealt extensively with the attraction forces domain between different surfaces and some liquids using the notion of cavitation in the surface process. Thus, is advanced a capillary force (Equation 6) relationship which produces the liquid movement from the contact zone towards the sample surface, in our case being a rough layer prominence [20].

$$F_{cap} = 4\pi\gamma\cos\theta R \left(1 - \frac{D}{\sqrt{\frac{v_{cap}}{\pi R} + D^2}} \right) \quad (6)$$

Where, R is the radius of a sphere with which we can approximate the peak prominence, D is the distance to the flat surface of the porous layer, θ is the contact angle, γ is the surface tension of the liquid, v_{cap} is the capillary volume.

Thus, the eluent reached on the profile peaks is adsorbed on their surface being moved toward the valleys of roughness and then it follows a displacement by capillary force of the eluent.

Regarding the causes of evaporation of the eluent in contact with the porous medium granules, this is due to the energy changes during the process of wetting of a porous solid when a certain amount of heat is liberated [22].

The two mechanisms discussed above cause the appearance a film of liquid (eluent) to rough surface that is beginning to move with the liquid to climb by capillary action through the porous of the plate TLC, the two tides of fluids comply to each other.

Roughness contributes to a particular flow of liquids on their surface. Many researchers have studied the spreading of liquid drops on porous surfaces or the flow on rough surfaces [23-26].

Hay et al. [26] proposed the invasive model of liquids displacement on rough surfaces, the invasive flow equation being (Equation 7):

$$x = Dt^{1/2} \quad (7)$$

Where, the constant of proportionality D is dependent on the method for estimating the roughness channel geometry, t being the displacement time of the front.

Each time, the frictional resistance is balanced against the driving force per unit area. Solving for the average velocity u of the front edge of the invading fluid yields (Equation 8) [26]:

$$u = \frac{\gamma d_h^2}{2P_0 \mu x} \left(\frac{(2\delta + \lambda) \cos\theta - \lambda \sin\theta}{\delta \lambda} \right) \quad (8)$$

where: d_h is hydraulic diameter; P_0 is Poiseuille number; γ is liquid- gas surface tension; λ is distance between cylinder edges (not centre to centre); δ is height of micronic cylindrical spikes (of theoretical model); μ is dynamic viscosity; t is the time it takes for the edge of the fluid to travel a distance x along the texture surface.

As it can be seen from Equation 8, the contact angle θ plays a great role in determining of the speed of the eluent. Marmur [27] cites Wenzel relationship established in the year of 1936 between the contact angle for the same liquid on a smooth surface and a rough surface (Equation 9),

$$\cos\theta_w = r \cos\theta_y \quad (9)$$

where θ_w is the apparent contact angle on the rough surface and θ_y is the ideal surface contact angle, and r is the ratio of the total area of surface roughness on the surface projection. A closer relationship of form roughness of this work is proposed by Hay et al. (Equation 10) [26]:

$$\theta_c = \arctan\left(\frac{2\delta}{\lambda} + 1\right) \quad (10)$$

where θ_c is a critical contact angle. If real θ is larger than θ_c , the fluid will not invade; if θ is smaller than θ_c , the fluid will invade.

By assimilating δ with maximum profile peak height (Rp) of 4.867 μm of the assessed profile, and λ with mean width (RSm) of 0.064 mm of the assessed profile, were introduced in equation 9, and was obtained $\theta_c = 52^\circ 30'$.

This means, according to Table XLVI of Bikerman's work [28] that low-aromatic liquids ($\theta = 49^\circ 40'$) will invade rough surface and high-aromatic liquids will invade both surfaces, smooth and rough. It can be concluded, according to Bikerman's theory that every groove, valley or scratch on a solid surface act as a capillary tube in which the liquid rises if the contact angle is less than 90° or descends if this angle is greater than 90° . Hence, a rough surface usually is better wetted than a smooth surface by a well-wetting liquid, while a poorly wetting liquid should spread on a smooth surface better than on a rough one [28].

Characterization of the surface of glass plates roughness (mat)

In our experiments we studied the surface characteristics of the two mat plates, Plate 1 and Plate 2, using atomic force microscopy (AFM) and a surface roughness tester. Figure 2 shows the AFM images obtained for the two mat plates, Plate 1 and Plate 2.

It can be observed that the tilt angles of profiles differ from Plate 1 ($32\text{--}51^\circ$) to Plate 2 ($11\text{--}15^\circ$), this aspect can influence the access of the eluent from the TLC plate, towards roughness plate. Since AFM has limitations regarding the maximum extension of the z scanner, we used the roughness tester for measure the surface parameters (RSm) of the two rough plates, Plate 1 and Plate 2, according to ISO 4.287-1997.

Thus, it measured the height of prominence (peak height profiles, Zp) and maximum depth of roughness (profile depth Valey Zv). The sum of the two parameters for two orthogonal directions was 11.260 μm and 11.044 μm respectively, for both mat glasses, differing only on the angle of rough surface profiles. By using the maximum height of profiles Rp = 4.867 μm and with the average width of profile elements RSm = 0.064 mm measured by roughness tester, were calculated the slope profiles and the similar values with those obtained by AFM method.

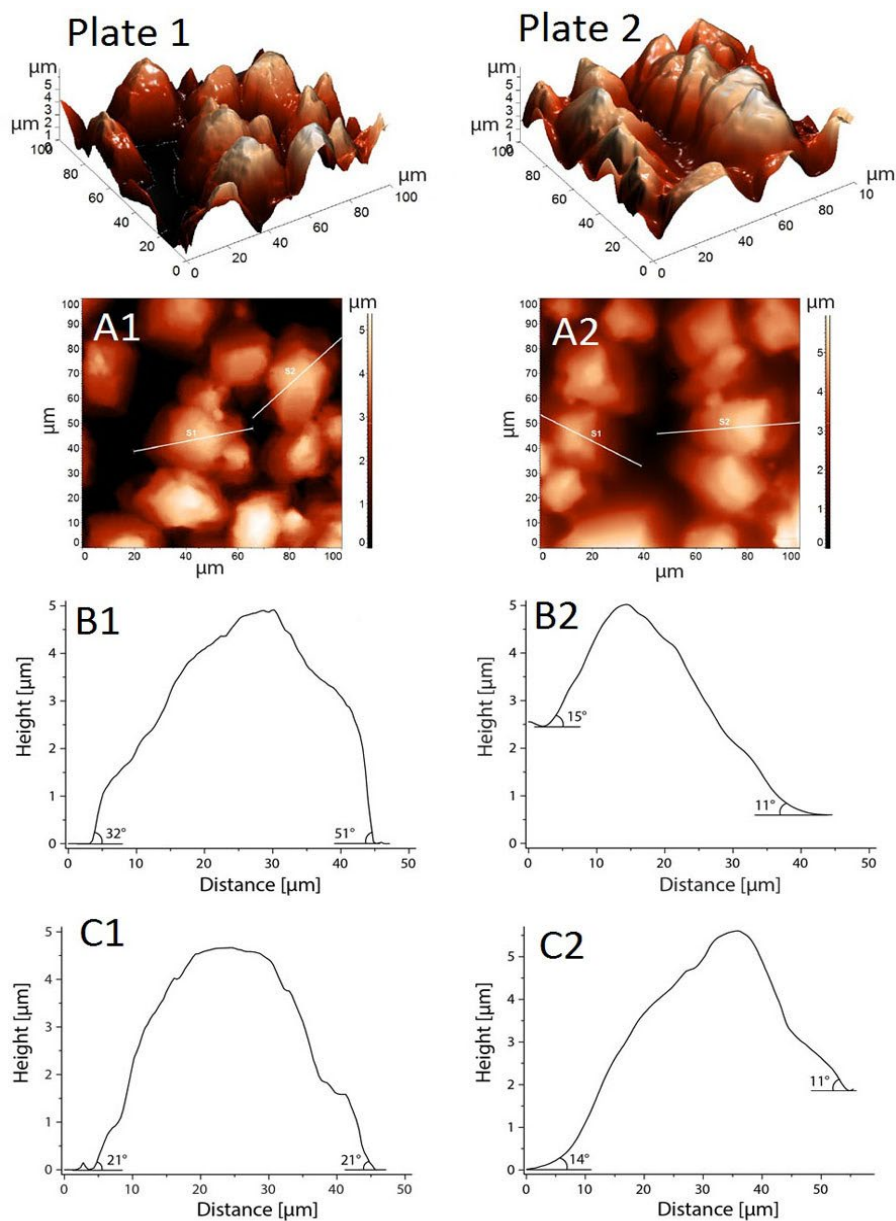


Figure 2. (A1, A2) 2D AFM images of the Plate 1 and Plate 2. (B1, B2) Section profiles corresponding to the white lines S1 highlighted in the 2D images. (C1, C2) Section profiles corresponding to the white lines S2 highlighted in the 2D images. Scan size 100 μm .

The TLC plates covered with the roughness plates (mat plate) are placed at an angle of 60° to the horizontal (Figure 1 II), hatched areas of roughness (Figure 2) being arranged differently from TLC area. The calculation showed that a molecule eluent that reached a prominent rough surface of the plate 2 is driven by a gravitational force of about 2.5 times higher than on a rough plate 1, rushing to filling the volumes of roughness and consequently enhance the flow speed of the eluent on the rough surface 2.

Migration of the eluent front on mat glass plate

Prior to measuring the speed of the eluent front on a porous surface as TLC type in combination with a rough plate, we were concerned about the form taken by the liquid front on the mat glass plate. For this purpose, the mat glass plate was placed over a smooth glass plate, as in Figure 1 I, but without free space (area labeled h parameter as in Figure 1 II). The methanol was use as mobile phase for determination of speed of eluent on a porous surface because it has less viscosity than the aromatic solvents used in chromatography.

The aspect of the eluent front on the mat glass plate shows fractal developments that were observed as described by Mandelbrot [29] and Dick [30].

It is obvious that the front line of the eluent in the TLC separations must be straight and that must be checked it in the following experiments. Also, the measurements of the velocity of the eluent front in our conditions has a great importance. Belenkii et al. [18] have drawn attention to the fact that, a possible way of increasing the effectiveness of TLC, is to decrease the elution rate. In this paper we aimed to find a practical method for the adjustment of the eluent velocity displacement.

In the first set of experiments, the TLC plate was covered with the mat glass plate, with rough surface of two qualities (see Figure 2), the lower edges of the plates being on the same level ($h = 0$, see Figure 1 II). A TLC plate of Al_2O_3 , activated at $105^\circ C$ for 30 minutes and benzene as eluent were used (Figure 3).

In Figure 3 I) are represented the average instantaneous velocity curves: a - the velocity curve of the eluent front, when TLC plate was put directly into the development chamber, as in the classical method; b - the velocity curve of the eluent front when the TLC plate was covered with the mat glass Plate 1; c - the velocity curve of the eluent front when the TLC plate was covered with the mat glass Plate 2;

Figure 3 I) shows that the front eluent velocity is significantly increased by covering the TLC plate with the mat glass plates. The highest value of front eluent velocity has been registered in the use of the Plate 2, contributing to the profile peaks.

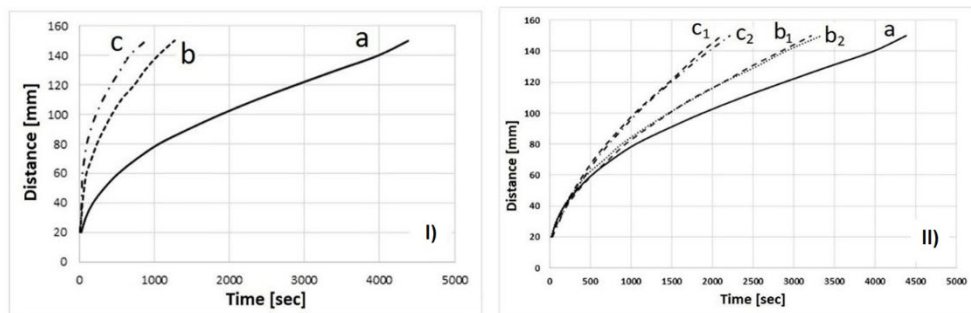


Figure 3. I) Influence of the mat glass plates superimposed on TLC plates on the velocities the eluent front; **II)** Influence of h free zone on the velocities of the eluent front.

The influence of free space h , the free zone of porous layer, (see Figure 1 II) was tested in order to reduce the speed of the front eluent. Thus, two lengths for h of 10 and 20 mm have been chosen, so that the evaporation surface of the eluent in the input differ significantly.

Figure 3 II) presents the velocity curves obtained by modification of values of h parameter. Where a - is the velocity curve of the eluent front, when TLC plate was immersed directly into the development chamber, as in the classical method; b_1 , b_2 - are the velocity curves of the eluent front when the TLC plate was covered with the mat glass Plate 1 (b_1 , $h = 10$ mm; b_2 , $h = 20$ mm); c_1 , c_2 are the velocity curves of the eluent front when the TLC plate was covered with the mat glass Plate 2 (c_1 , $h = 10$ mm; c_2 , $h = 20$ mm).

In this experiment, the arrangement of curves were maintained. Thus, the flattest curve was obtained for TLC plate exposed normally, then following for TLC plates covered with mat glass plates. The steepest curves were carried out with TLC plates covered with mat glass Plate 2.

Thus, it can be observed that by using the same type of mat glass plates, the average velocity drops, when h parameter is greatest, evaporation in the free zone having a braking effect over the eluent front.

During the chromatographic separations, a deformation of the eluent front was observed, in a parabolic shape with the tip down. This non-uniform shape of the front is a major disadvantage in TLC separations, with the eluent velocity being lower in the center of the plate and higher at the side edges of the plate.

The cause of this phenomenon is the counterpressure effect that the rough glass plate exerts on the displacement of the eluent vapors and implicitly on the eluent. In this way, on the side of the plate the vapors are released (escaped, lost, etc.) the speed of the eluent being higher than in the center of the plate.

This deficiency was corrected by scratching the porous layer, up to the level of the TLC plate glass, making 10 mm wide segments bordered by grooves. As a result, the vapor pressure of the eluents is equalized, the front is straight, but maintaining the advantages of this separation technique, with the overlapping of rough glass plates.

All the densitograms presented below were measured on scarified plates according to the above procedure. Scarification of TLC plates is an essential feature of the MG-TLC technique.

The chromatographic separation tests using the MG-TLC technique

For MG-TLC separation of the lipophilic compounds we used a colorants mixture test of Indophenol blue, Sudan red, and 4-Dimethylaminoazobenzene that was eluted with toluene, using silica gel TLC plates covered with the mat glass plates (Plate 1, Plate 2), using h free zone of 20 mm (Figure 1 II).

The separation was performed at 21°C room temperature and the solutes were spotted at 25 mm from lower end of the TLC plates. After MG-TLC development, the compounds densitograms (Figure 4) were achieved with densitometer at 450 nm.

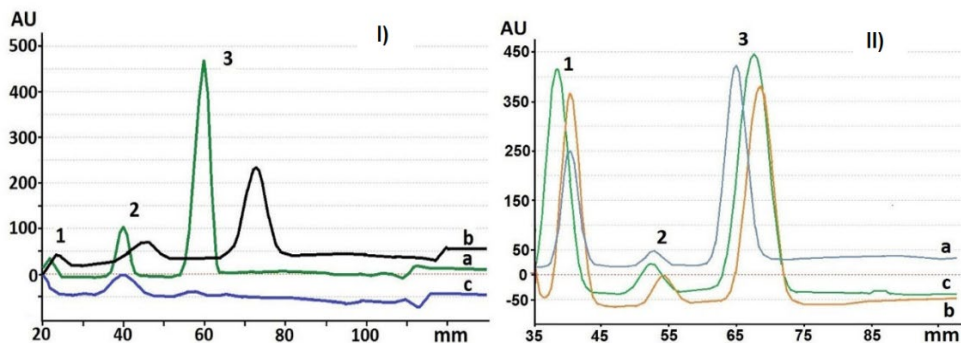


Figure 4. I) MG-TLC densitograms of lipophilic compounds (1 - Indophenol blue; 2 - Sudan red G; 3-4-dimethylaminoazobenzene) on silica gel plate (a - standard TLC; b - MG-TLC using Plate 1; c - MG-TLC using Plate 2); **II)** MG-TLC densitograms of hydrophilic compounds (1 - brilliant blue, 2 - carmoisine, 3 - tartrazine) on RP-C18 silica gel plate (a - standard TLC; b- MG-TLC using Plate 1; c - MG-TLC using Plate 2).

The overlapped densitograms of the MG-TLC chromatographic separation of lipophilic compounds are represented in Figure 4 I).

The separation results were comparing by using the R_x parameter [14] according to Equation 11:

$$R_x = \frac{\text{migration distance of substances in sandwich chamber}}{\text{migration distance of substances in standard chamber}} \quad (11)$$

The resolution was calculated using the following Equation 12 [31].

$$R_s = 2 \frac{\Delta z}{w_1 + w_2} \quad (12)$$

Where, Δz is the distance of migration between two spots, w_1 ; w_2 are widths of spots.

In Table 1 the values of solutes displacements x_{S1} , x_{S2} , x_{S3} in the three situations, R_x values (R_{X1} , R_{X2} , R_{X3}) are listed calculated according to the relationship (Equation 11). The resolutions of two neighbor peaks (R_{S1-2} , R_{S2-3}) were calculated and presented in Table 1.

Table 1. Chromatographic separation parameters of lipophilic compounds

Parameter	TLC standard	MG-TLC Plate 1 / TLC plate	MG-TLC Plate 2 / TLC plate
x_{S1}	5.50	8.00	4.50
x_{S2}	14.00	15.00	13.00
x_{S3}	39.00	44.00	45.00
X_{front}	69.00	78.50	81.50
R_{X1}	-	1.45	0.69
R_{X2}	-	1.07	0.93
R_{X3}	-	1.13	1.08
R_{front}	-	1.14	1.19
R_{S1-2}	2.09	2.19	1.19
R_{S2-3}	1.89	1.78	1.82

The chromatographic results show, by comparison with the TLC standard, a better separation for MG-TLC with Plate 1, although the eluent front has migrated less than in the case of MG-TLC with Plate 2. Thus, Belenkii's hypothesis were verified [18].

Based on the densitograms from Figure 4 a) the compounds separability in these three cases were calculated. According to Table 1 the best resolution of the separation for lipophilic compounds was obtained between compound 1 and compound 2 (R_{S1-2}) in the case of MG-TLC chromatography with Plate 1 and between compound 2 and compound 3 (R_{S2-3}) in the case of using TLC standard chromatography.

For MG-TLC *chromatographic separation of hydrophilic compounds*, we used the food dyes test: brilliant blue, carmoisine and tartrazine. The mobile phase used was mixture of water, acetone and ammonium sulphate (70 : 30 : 6.6 v/v/g) and as porous medium the plate RP-C18 silica gel plates on aluminum foil was used.

In Figure 4 II there are represented the overlapped densitograms of the MG-TLC chromatographic separation of hydrophilic dyes mixture measured at 450 nm. Chromatographic development time was 1 hour, the length of h free zone 10 mm, the starting point of the solvents was placed at 20 mm from the end of TLC plates. The first solute has not been moved from the starting point, so, R_x everywhere is equal to 1.

Table 2 presents the chromatographic separation parameters (solutes and front displacement and R_x calculation, according to the Equation 11 of hydrophilic dye mixture on studied chromatographic plates. Also, the resolution values of neighbor peaks were presented.

Table 2. Chromatographic separation parameters of hydrophilic compounds

Parameter	TLC standard	MG-TLC Plate 1 / TLC plate	MG-TLC Plate 2 / TLC plate
x_{S1}	0	0	0
x_{S2}	19.00	23.00	19.00
x_{S3}	39.00	49.00	47.50
x_{front}	90.00	93.00	93.00
R_{X1}	-	1.00	1.00
R_{X2}	-	1.21	1.00
R_{X3}	-	1.25	1.22
R_{front}	-	1.03	1.03
R_{S1-2}	1.79	1.89	1.75
R_{S2-3}	1.75	1.85	1.58

It can be shown that the best separation is obtained for the case of MG-TLC Plate 1 placed over the TLC plate. The resolution value greater than 1.5 shows a good separation of the peaks [14,31].

Other consideration relevant in MG-TLC

Among other effects at MG-TLC method (increased capillary force of the solvent, the absence of solvent evaporation, etc.) appear a specific effect, namely changing of equilibrium coefficient (K , equation 13), between the

concentration of a solute A in the stationary phase c_s , and the concentration of a solute A in the mobile phase, c_m :

$$K = \frac{c_s}{c_m} \quad (13)$$

In this case, due to the additional volume of the eluent provided by rough surface of the mat glass, the equilibrium concentration c_m changes and decreases in different way from one solution to another, this fact influencing the substances separability. A very suggestive graphical representation is provided by Bauer et al. [14].

CONCLUSIONS

The theoretical and practical aspects of the new method namely Mat Glass - Thin Layer Chromatography and application of invasion model was presented in this study. Some phenomena that occur in MG-TLC like, process flow, spreading on mat glass surface, impregnation of porous layers, chromatographic separation, etc., were developed and clarified. The practical aspect of MG-TLC method was supported by the good results obtained in separations of the lipophilic dyes and the hydrophilic dyes by small adjustments made, e.g. h height of the free zone of porous layer, or the roughness of glass plates. In our study the best separations have been obtained for the case of using the model of MG-TLC Plate 1 placed over the TLC plate, that has the contact angle on the rough surface higher than the buffer plate, Plate 2. The obtained results demonstrate that this method can be successfully used in TLC separation technique.

EXPERIMENTAL SECTION

Chemicals and Materials

TLC plates (ready-to-use layers for TLC), Sil G-25 UV254+366 and Alugram RP-18W/UV254, 20 x 20 cm purchased from Macherey-Nagel GmbH & Co. KG (Duren Germany) were sectioned into 3 strips (size 6.65 x 20 cm) and suitable in width with the available mat glass plates width. All reagents were of analytical grade. Toluene, benzene, acetone, were purchased from Merck (Darmstadt, Germany). Methanol and ammonium sulphate were purchased from Chimopar (Bucharest, Romania); For study the influence of the velocities

the eluent front in TLC sandwich chamber it was used the ALOX-25 UV254 (Al₂O₃) plate purchased from Macherey-Nagel GmbH & Co. KG (Duren Germany). Two types of test dyes mixture were purchased from Merck (Darmstadt, Germany): lipophilic dyes mixture (Indophenol blue, Sudan red and 4-Dimethylaminoazobenzene) and hydrophilic dyes mixture (Brilliant blue, Carmoisine and Tartrazine). Two types of mat glass plates were purchased from the specific market with the size 11 x 12.5 x 0.38 cm.

Equipment and Method

A roughness tester TR-220 (Maastricht, Netherlands) were used by measured the longitudinal and cross roughness of mat glass plates according to ISO 4287-1997. An atomic force microscope NT-MDT Ntegra Spectra (Moscow, Russia) in upright configuration, under ambient conditions, using NSG30 cantilevers (NT-MDT) with a typical resonant frequency of 320 kHz, force constant $k = 40$ N/m and tip curvature radius 6 nm (<10 nm) were used to measure the shapes of the prominences and profiles slopes of mat glass plates.

The chromatographic separation was performed in a normal chromatographic chamber. Samples of 2 μ l were manually applied at 2.5 cm to the bottom of the plate by means of a 5 μ l micropipette with ring mark (Duran, Germany) and the spots were dried in air before and after development. Densitometry scanning was performed with a Desaga CD-60 densitometer (Germany) at 450 nm in reflectance-absorbance mode.

ACKNOWLEDGMENTS

The authors would like to thank to Mr. Dr. Ing. Popa Grigore from Technical University of Cluj-Napoca, Laboratory of Measurements of the Surface Quality for measurements of the roughness of mat glass plates used in our experiments.

REFERENCES

1. Sz. Nyredy, *Planar chromatography. A retrospective View for the Third Millenium*, Springer, Budapest, **2001**.
2. I. Malinowska, J. K. Różyło, *J. Planar Chromatogr. - Mod. TLC*, **1998**, *11*, 411-414.
3. V. Coman, S. Kreibik, *J. Planar Chromatogr. - Mod. TLC*, **2003**, *16*, 338-346.
4. V. Coman, S. Kreibik, M. Vlassa, *J. Planar Chromatogr. - Mod. TLC*, **2008**, *21*, 373-377.

5. V. Coman, S. Kreibik, C. Tudoran, O. Opris, F. Copaciu, *J. Planar Chromatogr. - Mod. TLC*, **2012**, 25, 504-508.
6. E. Barrado, J. A. Rodriguez, *J. Chromatogr. A*, **2006**, 1128, 189-193.
7. I. Malinowska, M. Studziński, H. Malinowski, *J. Planar Chromatogr. - Mod. TLC* **2008**, 5, 379-385.
8. E. Tyihák, E. Mincsovics, *J. Planar Chromatogr. - Mod. TLC*, **2010**, 23, 382-395.
9. E. Tyihák, E. Mincsovics, *Nat. Prod. Commun.* **2011**, 6, 719-732.
10. B. Monaghan, *International Labmate*, Ltd XXXIII, **2007**, 2-6.
11. V. Coman, S. Kreibik, M. Vlassa, F. Copaciu, I. Perhaita, M. Filip, *J. Planar Chromatogr. - Mod. TLC*, **2016**, 29, 45-58.
12. E. Reich, A. Schibli, *J. Planar Chromatogr. - Mod. TLC*, **2004**, 17, 438-440.
13. V. G. Berezkin, E. V. Kormishkina, *J. Planar Chromatogr. - Mod. TLC*, **2006**, 19, 81-84.
14. K. Bauer, L. Gros, W. Sauer, *Thin Layer Chromatography. An Introduction*. Huthig Buch Verlag, Heidelberg, **1991**.
15. S. J. Gregg, K. S. W. Sing, *Adsorption, Surface Area and Porosity*. Academic Press, London, New York, **1967**, pp. 152.
16. R. C. Daniel, J. C. Berg, *Adv. Colloid Interface Sci.*, **2006**, 123-126, 439-469.
17. G. Guiochon, A. Siouffi, *J. Planar Chromatogr. - Mod. TLC*, **1978**, 16, 598-609.
18. B. G. Belenkii, V. I. Kolegov, V. V. Nesterov, *J. Planar Chromatogr. - Mod. TLC* **1975**, 107, 265-283.
19. C. F. Poole, *J. Planar Chromatogr. - Mod. TLC*, **1989**, 2, 95-98.
20. M. Wåhlander, P. M. Hansson-Mille, A. Swerin, *J. Colloid Interface Sci.*, **2015**, 448, 482-491.
21. P. M. Hansson, Y. Hormozan, B. D. Brandner, J. Linnros, P. M. Claesson, A. Swerin, J. Schoelkopf, P. A. C. Gane, E. Thormann, *J. Colloid Interface Sci.*, **2013**, 396, 278-286.
22. A. E. Scheidegger, *The Physics of Flow Through Porous Media*. University of Toronto Press, Toronto, **1960**, pp. 202.
23. V. M. Starov, *Adv. Colloid Interface Sci.*, **1992**, 39, 147-173.
24. V. M. Starov, S. R. Kosvintsev, V. D. Sobolev, M. G. Velarde, S. A. Zhdanov, *Adv. Colloid Interface Sci.* 2002, 246, 372-379.
25. K. M. Hay, M. I. Dragila, *Int. J. Numer. Anal. Model.* **2008**, 5, 85-92.
26. K. M. Hay, M. I. Dragila, J. Liburdy, *J. Colloid Interface Sci.*, **2008**, 325, 472-477.
27. A. Marmur, *Langmuir*, **2004**, 20, 3517-3519.
28. J. J. Bikerman, *Surface Chemistry. Theory and Applications.*, Academic Press Inc. Publishers. New York, **1958**, pp. 352-353.
29. B. B. Mandelbrot, *Les objets fractals: forme, hasard et dimension*. Flammarion Publishing, Paris, **1975**.
30. O. Dick, *Fractal Vision: Putting fractals to work for you*. Sams Publishing, Carmel, In, **1992**, pp. 287.
31. V. R. Meyer, *Practical High Performance Liquid Chromatography.*, John Wiley & Sons, Chichester, New York, **1998**, pp. 23.